Chapter 3

COMPOSITION CONTROL IN AN ENGINEERED MULTI-MEMBER COMMUNITY

3.1 Introduction

Microbial communities are everywhere and perform critical functions for the health of ecosystems at every scale. When environments change, community species compositions change, but we cannot predict changes or prevent them without greater knowledge of microbial communities and community control technology.

Bioengineers in various fields recognize the importance of microbial community control for different reasons. Genetic circuits in synthetic biology are constrained in their complexity by the burden they impose on cells; increasing the complexity of genetic circuits requires the distribution of circuit burden across a heterogeneous community of microbes [41, 42]. Additionally, genetic circuits operating independently in each cell of a population lose precision due to cell-to-cell variations in the population [43, 44]. Control of community composition and gene expression dynamics are required to create a stable platform for reliable circuit function.

Industrial bioproduction engineers recognize the efficiency and yield gains to be made by distributing production processes across a community of organisms [45, 46]. Systems dividing labor across a community outcompete monoculture only in specific systems optimized for minimal process bottlenecking across the community and ideal productive community composition, necessitating precise, stable control of community composition [47–49].

Ecologists and microbiologists learn more about natural microbial diversity through community control experiments mimicking natural ecologies. Community control deployed in native community environments has the potential to remediate and preserve natural microbial diversity [50, 51].

Acknowledging the growing truth that microbial community composition is integral to important topics like human health and industrial production, synthetic biologists have built circuits to take control of community composition itself.

The processes underlying community composition control are: intercellular signaling communicating population density and composition, information processing to

convert signals into appropriate community control action, and actuation of composition change using regulators of cell growth or death.

Scott *et al* created a two strain community that avoids collapse to a single strain monoculture. Each strain in the community expresses an identically structured, but independent genetic circuit that causes it to go through periodic bursts of growth and lysis. An orthogonal AHL checmical is produced by each strain which induces positive feedback production of more AHL, but also induces expression of the ϕX174E lysis protein [54]. At a critical concentration of AHL chemical, each strain lyses itself until its density is low and AHL levels decrease. While not implementing a precise form of community composition control, this circuit can prevent the decay of the two-strain coculture to a single strain monoculture over long culture times, even when growth rates or inoculation ratios are greatly mismatched.

Balagaddé *et al* created a circuit producing similar oscillatory growth dynamics, this time linking the member strains together with AHL chemicals, rather than leaving them to grow independently. Their circuit produces the out of phase growth dynamics characteristic of a predator-prey relationship, modeling a natural ecological relationship [58]. The predator strain kills the prey strain by producing an AHL signal that induces expression of ccdB toxin in prey, killing them. The prey strain "feeds" the predator strain by producing an orthogonal AHL signal that induces ccdA antitoxin in the predator. The predator strain constitutively produces ccdB, meaning predator strain growth is always limited by toxin without the prey inducing ccdA antitoxin. With the plethora of growth regulatory systems available, there is more than one way to tie predator growth to the prey: an auxotrophic predator strain fed by a metabolite-secreting prey strain could achieve the same goal. This circuit finds new functional space for community control circuits by using a toxin and antitoxin together to both up and downregulate strain growth.

Other circuits maintain cocultures using a genetic circuit only expressed in one strain. Dinh *et al* created a circuit to gradually decrease a strain's growth rate by degrading the early glycolytic enzyme phosphofructokinase A in response to AHL chemical [55]. Grown in coculture with an uncontrolled strain, the circuit-expressing strain will never outcompete its partner strain even if it dominates at inoculation; its growth slows before maximum population density is reached and the partner strain can grow into the community. While this coculture does not have oscillatory dynamics, the coculture composition is not stable. Over time, AHL accumulation will slowly decrease growth rate in the circuit-expressing strain,

eventually the uncontrolled strain will slowly overtake the culture.

Stable community compositions can be achieved using a completely different set of parts. Kerner *et al* created a coculture of auxotrophic E. coli whose growth rate and composition can be precisely tuned by the expression of metabolite export proteins [15]. The mutual dependence created by auxotrophy ensures that this community will eventually reach some composition steady state, tunable by the rate of metabolite export from each strain, because each strain requires the presence of the other to survive.

We take a similar mutual dependency approach, but use the ccdB/ccdA toxin/antitoxin pair instead. In this circuit, we use our previously reported *cap and release* genetic circuit motif to design a two-member population whose genetic circuit produces population density and composition steady states set by inducer inputs. For its ability to control the composition of the community to a target ratio of A cells to B cells, or $A_{population} = \alpha B_{population}$, we call it the ***A=B*** circuit. Like in the ccdB/ccdA based synthetic predator prey ecosystem, strain growth in *A=B* is limited by ccdB expression in response to AHL, but in this case, both strains express symmetric circuits that limit their own growth, but rescue the growth limitation of their partner.

Like the cross-feeding circuit published by Kerner *et al*, the *A=B* design can also be called a "cross-protection mutualism", which has recently been shown to be the best community architecture for establishing stable steady state community composition in two strain communities [82]. The mutual dependence of each strain in our circuit on its partner for protection from toxin expression mimics the metabolic dependence of the strains from Kerner *et al*.

One of the factors limiting the scaling of multi-strain community control circuits to sizes above two strains is the availability of orthogonal signaling molecules. More than two orthogonal AHL signaling systems exist and auxotrophic bacterial strains exist deficient for considerably more orthogonal metabolites. However, signal systems may have significant crosstalk that will limit the design of synthetically controlled communities with membership on the order of native communities

Guided by an analysis of the *A=B* circuit's sensitivity to its parameters, we detail a screening strategy to search functional parameter space for this genetic circuit. Experimental tests of the circuit as well as models and simulation demonstrate a need for degradation of AHL signals to allow steady state stability and perturbation rejection. By acquiring a genetic part encoding the aiiA AHL degradase, we

implement tunable AHL signal degradation and explore its effects on the *A=B* circuit's performance. Our final implementation of the *A=B* circuit can successfully regulate the composition of a community, with interesting additional effects on total population density.

3.2 Results

Designing the *A=B* population control circuit using the *cap and release* motif

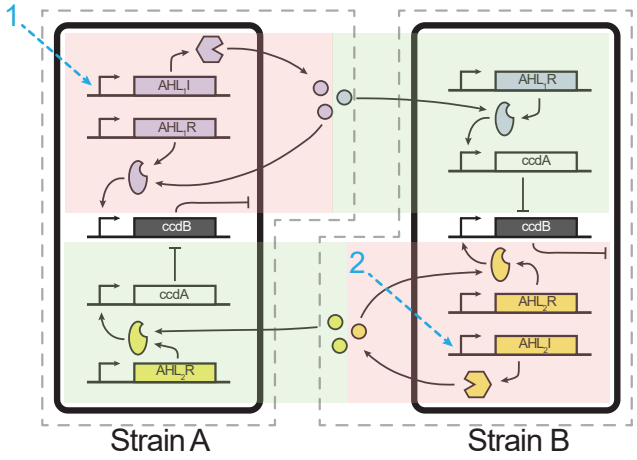

Figure 3.1: The A=B circuit uses a symmetric circuit motif in its two cells to create *cis*-acting negative feedback on each member and *trans*-acting rescues from negative feedback from each member to the other. "1" and "2" indicate genetic components that can be induced by the experimenter using IPTG and salicylate (sal), respectively.

In the *A=B* circuit, two inducers activate AHL production in each cell, signaling toxin production for each producer and antitoxin production for each partner (Fig.3.1). When AHL production is active, this architecture establishes an interdependence between the two strains where the loss of one strain would lead to the loss of the other due to unchecked toxin production. This interdependence is tunable by the experimenter: changing the level of each inducer pushes the system to new composition steady states (i.e. increasing inducer A produces more AHL A, reducing the A cell population and increasing B cell population). In the case where both inducers are at maximal levels, the *A=B* system is an implementation of the "cross-protection mutualism" detailed in Karkaria *et al* [82].

The specific components used in this implementation of *A=B* are described in Tables 3.1 and 3.2. In general, both strains contain *cap and release* circuit motifs (see Chapter 2). Strain A with negative population feedback driven by the Cin AHL system, release driven by Lux; Strain B with the opposite:

We created an ordinary differential equation model of the *A=B* system and simulated its composition control function. See Materials and Methods for description of parameters and variables. Subscripts 1 and 2 in the model correspond to the cell strains A and B, respectively.

$$\frac{dC_1}{dt} = k_C\left(1 - \frac{C_1 + C_2}{C_{max}}\right)C_1 - d_c C_1 \frac{T_1}{K_{tox} + T_1} - dC1 \tag{3.1}$$

$$\frac{dC_2}{dt} = k_C\left(1 - \frac{C_1 + C_2}{C_{max}}\right)C_2 - d_c C_2 \frac{T_2}{K_{tox} + T_2} - dC2 \tag{3.2}$$

$$\frac{dT_1}{dt} = \beta_{S_1}\left(\frac{S_1^2}{K_{S_1} + S_1^2}\right) + l_{S_1} - k_b A_1 T_1 - d_T T_1 \tag{3.3}$$

$$\frac{dT_2}{dt} = \beta_{S_2}\left(\frac{S_2^2}{K_{S_2} + S_2^2}\right) + l_{S_2} - k_b A_2 T_2 - d_T T_2 \tag{3.4}$$

$$\frac{dA_1}{dt} = \beta_{S_2}\left(\frac{S_2^2}{K_{S_2} + S_2^2}\right) + l_{S_2} - k_b A_1 T_1 - d_T A_1 \tag{3.5}$$

$$\frac{dA_2}{dt} = \beta_{S_1}\left(\frac{S_1^2}{K_{S_1} + S_1^2}\right) + l_{S_1} - k_b A_2 T_2 - d_T A_2 \tag{3.6}$$

$$\frac{dS_1}{dt} = \beta_{tac}\left(\frac{I^2}{K_{tac} + I^2}\right)C_1 + l_{tac} C_1 - d_S S_1 \tag{3.7}$$

$$\frac{dS_2}{dt} = \beta_{sal}\left(\frac{Sal^2}{K_{sal} + Sal^2}\right)C_2 + l_{sal} C_2 - d_S S_2 \tag{3.8}$$

Where C_x (mL^{-1}) represents the cell density of each strain in the population, T_x (nM) represents the average intracellular concentration of ccdB toxin in each strain, A_x (nM) represents the average intracellular concentration of ccdA antitoxin in each strain, and S_x (nM) represents the environmental concentration of each AHL signal (assumed to be equal inside and outside of cells due to free diffusion through cell membranes).

In eqs. 3.1 and 3.2 we model each strain's growth using a logistic model that compares the sum total population density with C_{max} to determine growth rate. Gene expression is never completely "off" when repressed or *not* activated, so in eqs. 3.3 - 3.8 we have included l_x terms to represent leaky expression of proteins (or the leaky synthesis of AHL signals caused by leaky synthase expression in the case of S_1 and S_2). To determine the value of each l_x parameter, we divide the corresponding β_x maximum production rate (describes the maximum production

rate of an inducible promoter) by the reported fold change of that promoter (all values sourced from [34]). All inducer molecule - transcription factor binding events are modeled with Hill equations. We also use a Hill equation to describe the increase in death rate with increasing toxin concentrations. Toxicity is not always modeled this way; sometimes death rate is assumed to be directly proportional to toxin concentration. Both are simplifying assumptions, the biophysical nature of toxicity is different for every toxin; more complicated models may attempt to capture this intricacy.

Table 3.1: Strain A components

Strain A		
Name	**Role**	**Description**
CinI	AHL_1 synthase	An enzyme that synthesizes Cin-type AHL chemicals (3-hydroxy-C14-homoserine lactone, 3-OH-C14-HSL) from S-adenosylmethionine (SAM) (amino donor) and an appropriate acyl–acyl carrier protein (acyl-ACP) (acyl donor). CinI is originally found in *Rhizobium etli* as part of the Cin AHL system, controlling nitrogen fixation and swarming motility [28, 83]. Cin AHL chemicals can freely diffuse through bacterial membranes, meaning their concentration in a mixed culture environment is equal both inside and outside cells.
CinR	AHL_1 TF	A transcription factor that binds Cin AHL molecules, dimerizes, then binds as a dimer-AHL complex to the pCin promoter, *activating* transription of downstream genes. **In Strain A, it activates transcription of ccdB.**
LuxR	AHL_2 TF	A transcription factor that binds Lux AHL molecules, dimerizes, then binds as a dimer-AHL complex to the pLux promoter, *activating* transription of downstream genes. **In Strain A, it activates transcription of ccdA.**
ccdB	toxin	A small 101 amino acid toxin protein expressed natively from the *E. coli* F plasmid *ccd* operon. ccdB covalently traps DNA gyrase in an unstable DNA strand-cleaved conformation [60, 61]. Stuck in this state during replication, the genome fragments and the cell dies.
ccdA	antitoxin	When present together with ccdB, ccdA binds ccdB with picomolar affinity [67], sequestering it and blocking its toxic activity. ccdA can bind and inactivate both free ccdB *and* ccdB already complexed with DNA gyrase; ccdA reverses ccdB/gyrase binding and restores gyrase to normal function.

To visualize the tunable composition control function of $A{=}B$, we can simulate two types of "virtual experiment". One simulates the growth of $A{=}B$ cocultures in identical inducer conditions, each starting from a different initial composition; the other simulates coculture growth in varying inducer conditions, starting from

Table 3.2: Strain B components

Strain B - AHL sythase and TFs regulating ccdB and ccdA swapped from Strain A		
Name	**Role**	**Description**
LuxI	AHL_2 synthase	An enzyme that synthesizes Lux-type AHL chemicals (3-oxohexanoyl-homoserine lactone, 3-O-C6-HSL) from S-adenosylmethionine (SAM) (amino donor) and an appropriate acyl–acyl carrier protein (acyl-ACP) (acyl donor) [59]. Lux AHL chemicals can freely diffuse through bacterial membranes, meaning their concentration in a mixed culture environment is equal both inside and outside cells.
CinR	AHL_1 TF	In Strain B, it activates transcription of ccdA.
LuxR	AHL_2 TF	In Strain B, it activates transcription of ccdB.

identical initial compositions. These simulations mimic two possible experiments that can be run to test the functions of $A{=}B$.

In the first simulated experiment (varying initial composition against constant inducer concentrations), we predict the ability of the system to drive cocultures from their initial compositions to the steady state composition encoded in the inducer concentrations. A perfect $A{=}B$ controller will drive all cocultures to the same final composition, regardless of initial composition.

In the second simulated experiment (constant initial composition with varying inducer concentrations), we predict the range of different composition steady states accessible to the controller, set by the unique combination of inducer concentrations. Ideally, the whole range of steady state compositions from 100% A cells to 0% A cells can be driven by this controller.

AHL signals communicate strain density information around the community and are also the only circuit components not contained inside cells. This means they are not diluted into daughter cells during division and—without components to do so—are not degraded by cellular machinery. Only their passive breakdown in the environment reduces their concentration over time. In each of these simulated experiments we will also explore the role of active cell-mediated AHL signal degradation. In the laboratory, we can implement such degradation using the aiiA degradase enzyme, whose expression can be induced in each cell. Without enzymatic AHL degradation, AHLs are assumed to passively degrade in the environment with rate d_S as in eqs. 3.7 and 3.8. To model enzymatic AHL degradation induced in each cell in the system, eqs. 3.7 and 3.8 become 3.9 and 3.10 listed below.

$$\frac{dS_1}{dt} = \beta_{tac}\left(\frac{I^2}{K_{tac}+I^2}\right)C_1 + l_{tac}C_1 - d_{sc}S_1\left(C_1+C_2\right) - d_S S_1 \tag{3.9}$$

$$\frac{dS_2}{dt} = \beta_{sal}\left(\frac{Sal^2}{K_{sal}+Sal^2}\right)C_2 + l_{sal}C_2 - d_{sc}S_1\left(C_1+C_2\right) - d_S S_2 \tag{3.10}$$

Where d_{sc} is the per cell AHL degradation rate mediated by aiiA enzyme. This value is arbitrarily set by the experimenter by changing the concentration of aiiA inducer. The true AHL degradation rate effected by each aiiA enzyme is not known, so we make do in simulation by scanning across many values for d_{sc} to observe its effects on the system.

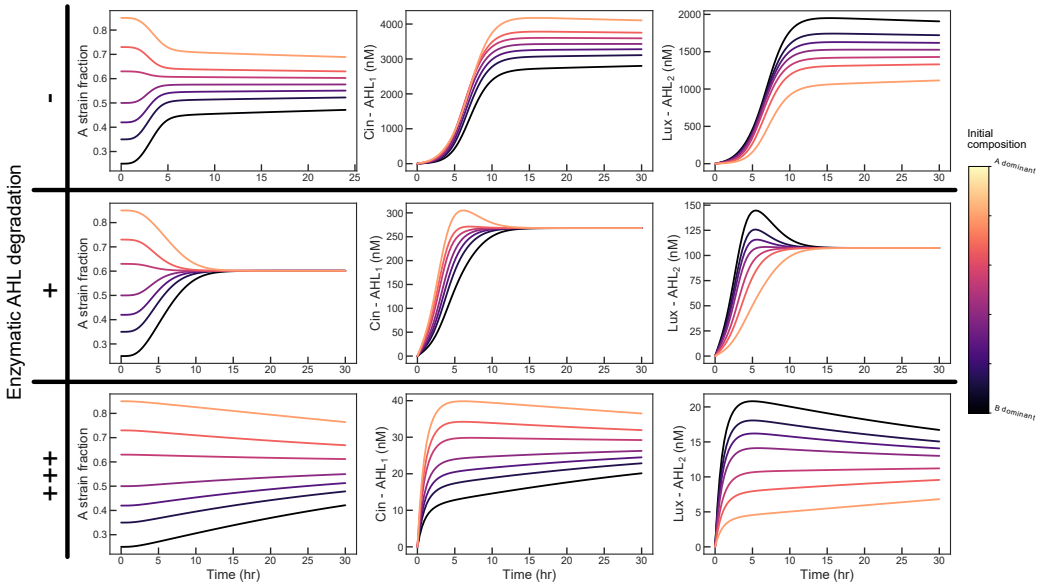

Figure 3.2: *A=B* sim experiment 1: varying initial compositions The *A=B* system was simulated starting at compositions varying from A strain dominated to B strain dominated. Per cell enzymatic AHL degradation was either OFF (TOP) or ON (MID) or ON+++ (BOTTOM) to observe the performance effects of increased AHL degradation.

Simulating *A=B* cocultures starting at varying initial compositions reveals the importance of AHL degradation to composition control performance (Fig. 3.2). Without enzymatic degradation (Fig. 3.2 TOP), the circuit begins to drive the cocultures to a steady state composition, but abruptly loses power, thereafter only very slowly bringing composition under control (steady state achieved at >400 hours). This loss of control performance precludes the establishment of a composition steady state in a realistic experiment (duration on order~days).

Both strains are induced to produce AHL strongly, in theory broadcasting the information necessary for composition control, but perhaps doing so too strongly. While a basal level of passive AHL breakdown is included in the model, it is not sufficient to stabilize AHL concentrations at useful levels against this strong production. Modeling passive AHL breakdown alone, both AHL signals accumulate to concentrations ~10-20x greater than their binding constants ($K_{S1} = 250nM$ and $K_{S2} = 100nM$ [34, 81]). These concentrations are well into saturating ranges in which changes in AHL concentration do not produce significant changes in gene expression from their associated promoters. As the coculture is growing and AHL signals are accumulating through concentrations near to their binding constants (hours 0-5), the circuit makes an incomplete attempt to drive each coculture to a steady state composition. As the AHLs saturate, the expression rate of actuators ccdB and ccdA reach their maxima, nearly balancing each other, inhibiting the ability of the circuit to push the cocultures to a steady state composition.

We simulate the enzymatic degradation of AHL in each cell by setting the per cell AHL degradation rate, d_{sc}, to a rate ~100x less than AHL production (Fig. 3.2 TOP). Now, the circuit is able to prevent AHL accumulation, quickly producing steady state AHL levels very close to their binding constants in all cocultures. In these concentration ranges, even the small differences in AHL concentration produced by each coculture are sufficient to functionally alter ccdB and ccdA expression to achieve a composition steady state.

We simulate extremely strong degradation of AHL by setting d_{sc} 10x higher, and find that *over*degradation of AHL is possible. At this rate of degradation, AHL signals begin to stabilize at concentrations ~ 10x lower than their binding constants. At these concentrations, ccdB and ccdA are not meaningfully activated and the circuit again has unreasonably slow control performance.

It is clearly important that we include the aiiA degradase in our laboratory implementation of *A=B* to control AHL accumulation and coculture composition.

In our second simulated experiment, we start each *A=B* coculture at the same composition (50% A strain, 50% B strain) and vary the inducer concentrations that direct AHL production from each strain. Intuitively, relatively strong production of AHL from one strain should push the coculture towards a composition dominated by the relatively weakly producing strain. We will again explore the effect of enzymatic AHL degradation.

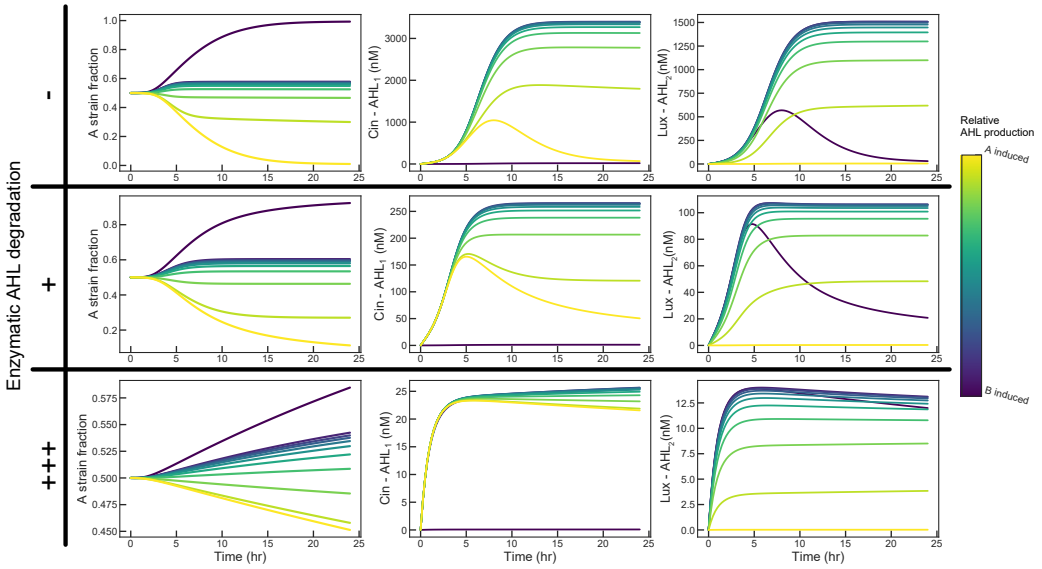

Figure 3.3: *A=B* sim experiment 2: varying AHL production from each strain The *A=B* system was simulated starting at a 1:1 strain composition with varying AHL production from each strain. Darker shades represent relatively more AHL production from strain B, lighter shades relatively more from strain A. Per cell enzymatic AHL degradation was either OFF (TOP) or ON (MID) or ON+++ (BOTTOM) to observe the performance effects of increased AHL degradation.

Even without enzymatic AHL degradation (Fig. 3.3 TOP), varying relative AHL production from each strain is capable of setting a variety of different composition steady states that are achieved in a reasonable amount of time. As we expect, progressively stronger AHL production from the A strain (lighter shades) pushes the coculture to a composition dominated by the B strain, and vice versa.

In the extreme cases of AHL production from only one strain (A (bright yellow) or B (dark purple)) the producing strain generates the only AHL in the system and kills itself until it drops out of the coculture. As it drops out, its AHL production wanes until the coculture becomes a monoculture and no AHL is produced at all (Fig. 3.3 TOP - center and right). When AHL production from each strain is approximately equal, balanced coculture compositions are produced.

Without enzymatic degradation, AHLs still accumulate to saturating concentrations by the end of the experiment. As the cocultures are growing, however, AHLs accumulate through concentrations near their binding constants and any imbalance in their accumulation rates still pushes the cocultures to different composition steady states.

With increasing AHL degradation by each cell (Fig. 3.3 MID and BOTTOM),

the same levels of AHL production produce more extreme compositions that are achieved more slowly. These simulations predict that AHL degradation will not affect the range of composition steady states available to the circuit, but will affect the composition produced at a given level of AHL production from each cell. There is still a risk of overdegrading AHL; too much AHL degradation dramatically slows the establishment of different compositions.

These two simulated experiments are models of experiments we can perform in the laboratory to learn whether a real implementation of *A=B* is functional.

Building the *A=B* circuit

The *A=B* circuit is actuated by the ccdB toxin, produced by each strain in response to its AHL signal, and sequestered by ccdA produced in response to the partner strain's AHL signal. The ccdB protein is a highly potent toxin and slight mis-expression can easily lead to total death of one strain (if ccdB is too strongly expressed) or the inability to cap a strain's growth at all (if ccdB is expressed too weakly). Most parameters in the circuit have a downstream effect on ccdB expression, so parameter ranges in which this circuit design is actually a functional controller are tight. Parameter sensitivity analysis [84, 85] performed with independent models of each cell strain reveals that the steady state density of each strain is sensitive to a few of the parameters in the model: $l_{S_{ccdA}}$ (l_{S_2} in strain A, l_{S_1} in strain B), basal leakiness of ccdA expression; $\beta_{S_{ccdB}}$ (β_{S_1} in strain A, β_{S_2} in strain B), maximal ccdB expression rate; k_C, cell growth rate; d_C, death rate constant for ccdB (ccdB potency); d, basal cell death rate (Fig. 3.4). Of all these parameters, only $\beta_{S_{ccdB}}$ (in model as β_{S_1} or β_{S_2}) is modifiable by we the experimenters; the others are constants inherent to the promoters, proteins and cells used.

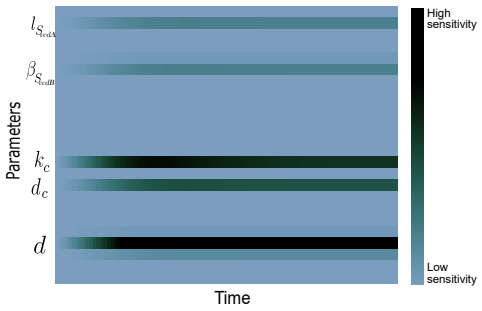

Figure 3.4: Sensitivity analysis of A=B strains reveals the stady state density of each cell strain is sensitive to a few model parameters. Sensitivity analysis performed by the methods described in [84, 85].

Thus, to create the functional circuit in the laboratory we chose to screen circuit variants with different ribosome binding site (RBS) strengths driving ccdB translation to

search the widest range of circuit functional space. Different RBS sequences change the rate at which ccdB mRNA is translated into protein, modifying the maximum rates of ccdB expression, β_{S_1} and β_{S_2}.

We used 3G assembly [12] to to first assemble plasmids A1 and B1 (Fig. 3.5). These plasmids contain all the invariant parts of each strain's circuit motif (AHL synthase, ccdA). These plasmids were transformed into Marionette Wild *E. coli* [34] to generate the basic chassis of the A and B strains. Note that this circuit assembly process *does not* include the aiiA AHL degradase. The resulting cells are not capable of enzymatic AHL degradation.

3G assembly was again used to create sets of A2 and B2 plasmids by assembling a pool of RBS sequences between each plasmid's AHL inducible promoter and the ccdB gene. This process should generate sets of A2 and B2 plasmids with each unique RBS from the pool represented in the set. These plasmid sets were transformed into ccdB resistant DB 3.1 *E.coli* to generate single colonies, each containing a unique A2 or B2 plasmid that could be amplified and isolated. A subset of these plasmids were purified and sequenced for use in experimentation. We purified four A2 and B2 plasmids each, then transformed the A1 and B1-containing chassis cells with each of the appropriate 4 A2 or B2 plasmids, generating 4 strain variants each (Fig. 3.5). Their number is drawn from their variant number and clone number (e.g. B42 indicates is was the **2**nd clone of the **4**th B2 plasmid transformed into B1 containing cells). Strain A is labeled by CFP expression from plasmid A2, strain B is labeled with YFP on plasmid B2.

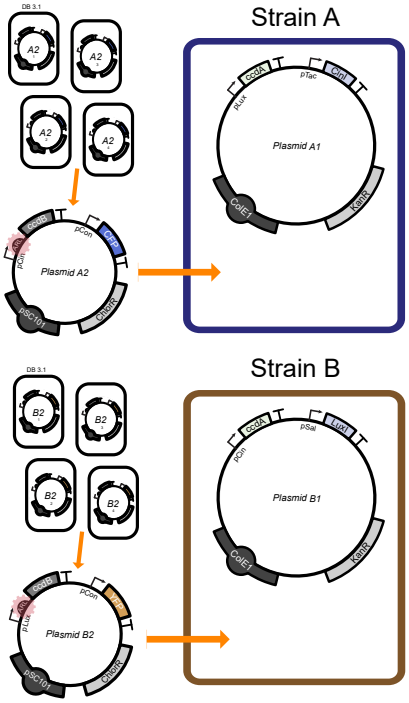

Figure 3.5: Method of generating A and B cell variants

Screening of the different ccdB expressing variants of each cell strain had 2 selection phases, a negative selection against variants overexpressing ccdB with an overpowered RBS and a functional screen for appropriate community behavior in a simple experiment observing coculture behavior with the circuit "ON"

(both strain inducers (IPTG, Sal) at maximal induction) and “OFF” (no inducers present).

The first phase is complete when viable A and B strain colonies appear after transformation with the A2 and B2 plasmids. Those that grow do not leak ccdB expression at a rate that is lethal to cells. In phase two, surviving A and B strain variants are mixed together and grown in both "ON" (1 mM IPTG, 30 uM sal) and "OFF" (0 IPTG, 0 sal) inducer conditions to check each community’s response to maximal AHL production and zero AHL production. Communities that collapse to monoculture in either induction condition were passed over as candidates for further testing.

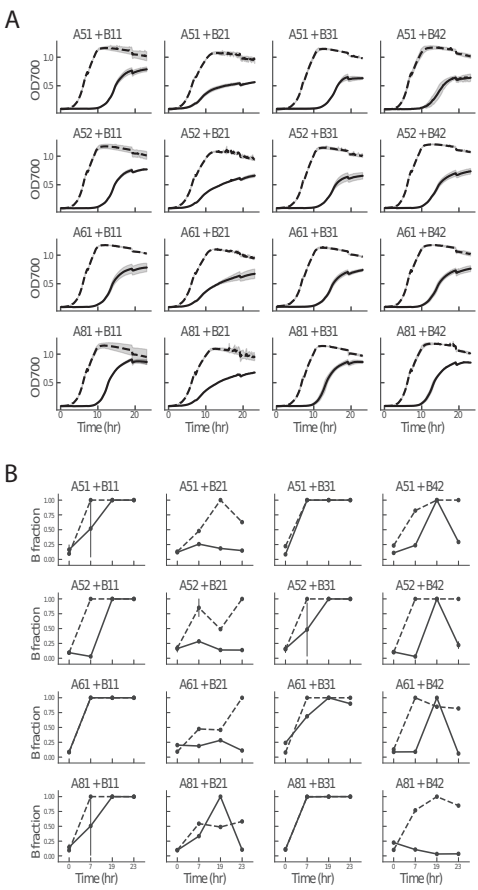

Figure 3.6: A=B screening results Mixtures of variants of each cell type scan parameter space, demonstrating that total density control is much more robust to parameter changes than composition control. Induced mixtures of cells are drawn as solid lines, uninduced mixtures are dashed. (A) Total community density measured by OD700 (B) Calculation of B strain fraction in the community from flow cytometry.

We know from the coculture of non-circuit-containing control bacteria that a coculture growing without any genetic circuit-based population control will maintain its initial composition over a growth phase (Fig. 3.10). We know from simulation that approximately equal AHL production from each strain in coculture should lead to the establishment of mixed composition at steady state, not a monoculture. Thus, our screen seeks to identify cocultures made of A and B cell variants that express ccdB at rates that will produce mixed compositions with full induction of A and B cell AHL production.

A note about the Marionette cell line used to generate the A and B strain variants: It contains a genome integrated cassette expressing 12 transcription factors whose responses to their inducers are completely characterized. From the data presented

in the supplement of Meyer *et al.* [34], we knew what concentrations of IPTG and sal to use to achieve maximal circuit induction (1 mM IPTG, 30 uM sal).

During community growth, total density was measured as OD700 in an incubator/plate reader. At four time points, samples were taken from each community, and analyzed with a flow cytometer. To separate bacteria from noise and dust in the flow cytometer, we stained each culture sample with ThermoFisher Syto 62 dye (catalog # S11344), which diffuses into cells (both live and dead) and stains nucleic acids with red fluorescence. Only the cytometry events with strong red fluorescence were passed through for determining community composition. Strain A's CFP expression was weak, providing little resolution between CFP^+ A cells and CFP^- B cells. Instead we made our community composition analysis using the YFP channel, assuming YFP^+ cells were B cells and YFP^- cells were A cells. A Gaussian mixture model was fit to the YFP channel cytometry data and used to assign events to either the narrow YFP^- or wide YFP^+ peaks. See Materials and Methods for a detailed description of cytometry gating strategies, data analysis and community composition computation.

Composition control was variable across the screened co-cultures (Fig. 3.6 B). Cocultures containing B11 and B31 did not appear to achieve different compositions in different inducer conditions, rather they nearly immediately collapsed to A cell monocultures in both inducer conditions. Cocultures containing B21 and B42 maintained mixed compositions that performed similarly in response to inducers, regardless of A strain variant. In general, the B strain variant seemed to determine the behavior of the coculture. Cocultures of interest included all those with variants B21 and B42. The strain variants in these cocultures were considered candidate functional strains and saved for more detailed testing.

Interestingly, where neither of our two simulated experiments predicted significant alterations in steady state population density due to circuit action (Fig. 3.11), a population density control phenotype was observed in all cocultures tested (Fig. 3.6 A). Every induced coculture's density was capped to 75-50% of its uninduced final density; again, the B strain seemed to determine the specific population capping dynamics observed. These results suggests that ccdB expression is outstripping ccdA expression when AHLs are produced in these cocultures.

Altogether the screening method we used was not as predictive or helpful as expected. The low time resolution and poor separation of CFP^+ and CFP^- A cells may have limited our ability to detect interesting composition control behaviors. The results

presented in the next section did not match the data generated in our screen. It is possible that the strains chosen for testing were simply lucky picks from the screening process or that the flow cytometry screen did not return accurate results.

Testing the *A=B* circuit—varying AHL production

With our saved strains, we hoped to demonstrate *tunable* population density and composition steady states by testing intermediate inducer concentrations between the binary "ON" and "OFF" used in the screening process. This experiment is a version of simulated experiment 2 in which we varied AHL production from each strain. We expect induction of AHL production from each strain to effect changes from the initial composition (Fig. 3.3). The effect is predicted to be observable even though these strains lack the ability to enzymatically degrade AHL.

We mixed the indicated cell strains together 1:1, then grew them in a set of 4 inducer conditions over which both inducer concentrations increased together. The cultures were grown for 18 hours, then diluted 1:10 in identical inducer concentrations to observe whether the initial steady states are maintained through another growth cycle. Every 10 minutes, we measured OD700, YFP and CFP in each culture. At 5 time points throughout the experiment, we also took samples of each coculture to determine viable cell counts (Fig. 3.7 A-B, *Right*)

We concurrently grew various control cultures to help estimate coculture composition from CFP and YFP fluorescence values. The control cultures were simply monocultures of each strain tested—monoculture A61, monoculture B21, monoculture B42—grown from the same starting density as the mixtures in the same inducer concentrations. For these control monocultures, fluorescence was divided by OD700 at every time point to create a reference fluorescence/OD value that indicated how many fluorescence units to expect per OD unit for a culture composed entirely of CFP^+ B42 cells or YFP^+ A61 cells etc. Fluorescence/OD units were computed for each experimental coculture and compared to the same units from the control monocultures to estimate what fraction of that coculture was one cell strain or the other. The method is not completely precise, but provides very highly time resolve estimates of coculture composition. This method does not *directly* measure coculture composition, instead it computes two separate estimates of strain A/B population fraction by by comparing coculture fluorescent output to the output from two independent A or B strain monocultures. This is why both blue (A strain) and yellow (B strain) population fraction estimates are plotted in (Fig. 3.7 B *Left*),

because the estimate of A strain population fraction does not imply B strain fraction and vice versa. Because cocultures are composed of *only* blue - A or yellow - B cells and viable cell counting directly visualizes and quantifies both strains, A cell fraction implies B cell fraction (1 - A_{frac}). As a result, only A fraction is displayed for clarity.

Where AHL degradation is not required for setting different composition steady states by varying AHL production from each strain, AHL degradation is required for rejecting perturbations to composition steady states (Fig. 3.12). The dilution of the tested cocultures does not explicitly perturb composition, but does perturb population density. Because the strains in these cocultures cannot degrade AHL, we do not expect them to reject any perturbations to composition produced by dilution.

Population density of both cocultures was capped at or below OD700 1.0 during the first 18 hour growth phase in all inducer conditions (Fig. 3.7 A *Left*). The lowest inducer concentrations (IPTG 100 uM, Sal 5 uM) produced the strongest cap on steady state density, where the densities produced by the other induction conditions were not distinguishable from that of the uninduced condition. This trend was common to both cocultures. In the second growth phase after the 1:10 dilution, density control appeared to be lost; both cocultures grew past their initial density caps to the carrying capacity of the vessel (OD700 1.4).

Viable cell counts revealed different total population density dynamics between the two cocultures ((Fig. 3.7 A *Right*) and Table 3.3). In the first growth phase, A61+B21 grew to densities on order 10^6 cells/mL, the uninduced coculture reached a density ~2x greater than the induced cocultures. In the second growth phase, A61+B21 in each inducer condition reached a density ~10x greater than its first phase steady state—density control was lost. Where OD700 did not detect significant differences in total population density at the end of the second growth phase in A61+B21, in any of the inducer conditions, viable cell counts revealed significant continuing effects of inducer on total population density. Generally, increasing inducer concentrations produced lower total density.

A61+B42 responded very differently after dilution. In the first growth phase, A61+B42 grew to densities on order 10^6 cells/mL without large differences between inducer conditions. However, at the end of the second growth phase, induced A61+B42 did not exceed its first phase density steady states to the great degree A61+B21 did. Uninduced A61+B42 grew past its first phase density by ~50x, but the induced cocultures grew to densities within 1-3x their first phase densities—

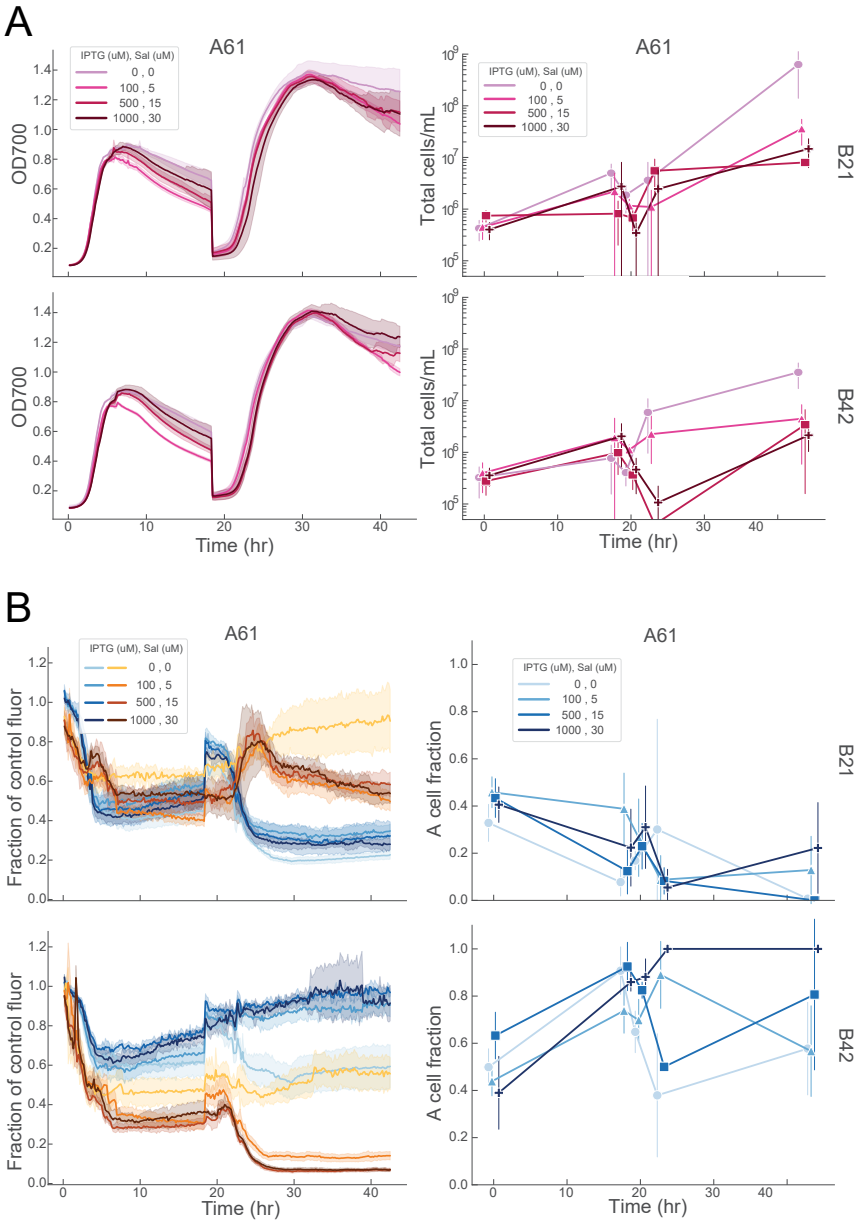

Figure 3.7: Tuning population density and composition with perturbation. Two cocultures composed of A and B cell variants A61, B21, B42 in all AB combinations were grown in increasing inducer concentrations. (A) Total population density measured using (*Left*) OD700 and (*Right*) viable cell counts. (B) Coculture composition analysis (*Left*) Two independent estimates of A and B population fraction from fluorescence measurements (*Right*) Population composition determined from viable cell counts using fluorescent strain labels. Because cocultures are composed of *only* blue - A or yellow - B cells and viable cell counting directly visualizes and quantifies both strains, A cell fraction implies B cell fraction (1 - A_{frac}. As a result, only A fraction is displayed.

density control may have been maintained through the perturbation.

A61 + B21		
IPTG, Sal	**Density steady state 1 - 18 hr**	**Density state 2 - 43 hr**
0 uM, 0uM	$4.89{\cdot}10^6$ cell/mL	$6.2{\cdot}10^8$ cell/mL
100 uM, 5 uM	$2.2{\cdot}10^6$	$3.6{\cdot}10^7$
500 uM, 15 uM	$8.0{\cdot}10^5$	$8.0{\cdot}10^6$
1000 uM, 30 uM	$2.7{\cdot}10^6$	$1.4{\cdot}10^7$
A61 + B42		
IPTG, Sal	**Density steady state 1 - 18 hr**	**Density state 2 - 43 hr**
0 uM, 0uM	$7.7{\cdot}10^5$ cell/mL	$3.5{\cdot}10^7$ cell/mL
100 uM, 5 uM	$1.9{\cdot}10^6$	$4.4{\cdot}10^6$
500 uM, 15 uM	$9.8{\cdot}10^5$	$3.4{\cdot}10^6$
1000 uM, 30 uM	$2.0{\cdot}10^6$	$2.1{\cdot}10^6$

Table 3.3: Coculture total viable cell counts

Each coculture was pushed to a different composition in response to increasing inducer concentrations (Fig. 3.7 B). Uninduced A61+B21 decayed quickly to B strain monoculture. Composition estimates from YFP and CFP data do not indicate this movement towards B strain dominance until after the dilution at 18 hours, though viable cell counts demonstrate this trend during the entire experiment. Induced A61+B21 behave similarly, cocultures in each induction condition decay to B strain monoculture with similar dynamics to the uninduced coculture.

Uninduced A61+B42 maintained its starting 1:1 population composition throughout the experiment according to both fluorescence-based composition estimates and viable cell counts. This is expected from an unregulated mixture of non-interacting cells (Fig. 3.10). Increasing inducer concentrations consistently pushed A61+B42 towards A strain dominance. Fluorescence measurements indicated nearly complete dominance of the A strain at the end of the experiment, regardless of inducer concentration, while viable cell counts suggest a possible dependence of final A strain population fraction on strength of induction. The large variance in viable cell counts may artificially produce this apparent relationship between final composition and inducer concentrations; more counts need be taken in the future to increase our confidence in composition measurements.

Adding AHL degradation to *A=B*

Using cocultures without the ability to actively degrade AHL, we expect AHL signals to accumulate into saturating concentrations, blunting composition control.

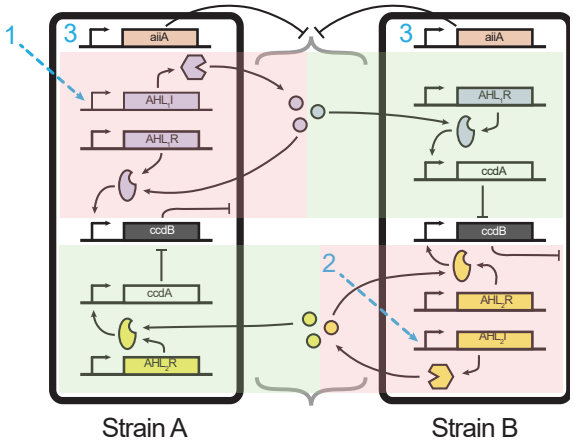

Figure 3.8: AHL degradation in the A=B circuit. (A) The aiiA degradase is added to both A and B strains under control of the pCau DHBA responsive promoter. It is placed on plasmids A1 and B1 as part of the invariant chassis of the A and B strains. (Inducer 1 = IPTG, AHL_1 = Cin AHL (3-hydroxy-C14-HSL), inducer 2 = sodium salicylate, AHL_2 = Lux AHL (3-O-C6-HSL), inducer 3 = 3,4-dihydroxybenzoic acid (DHBA)).

We considered two options for controlling AHL accumulation in our system: either physically dilute the coculture during an experiment to remove AHL—at the cost of regular perturbations of the system from steady state—or add active AHL degradation to the circuit.

Active AHL degradation is provided by the *Bacillus thuringiensis* gene *aiiA*, encoding a lactonase that promiscuously degrades AHL signals. Various *aiiA* DNA coding sequences can be found across microbiology [75] and synthetic biology literature [20, 86], but we found the originally deposited sequence (GenBank: AF196486.1) to work most reliably in our system [18]. We added aiiA expressing sequences to the A1 and B1 plasmids that form the invariant chassis for the A and B strains, both controlled by the pCau promoter induced by DHBA, so enzymatic AHL degradation could be induced from all cells in a coculture with one inducer (Fig. 3.8). Since AHLs diffuse across cell membranes, aiiA enzymes made inside cells will deplete AHLs from the total environment.

We combined *both* physical and enzymatic methods of AHL removal in one experiment to learn how they affect population control by the *A=B* circuit. We grew the A61+B42 coculture for 8 hours in a few inducer conditions: no induction, maximal A strain induction (1 mM IPTG), maximal B strain induction (30 uM Sal), maximal induction of both strains (1 mM IPTG, 30 uM Sal), max induction of both strains with aiiA induction (1 mM IPTG, 30 uM Sal, 1 mM DHBA). This experiment is again modeled after simulated experiment 2 in which cocultures at the same

starting composition are grown in different inducer concentrations to set different composition steady states.

Every hour each coculture was diluted 1:2. Before each dilution, samples of the coculture were removed for precise quantification by counting viable cells.

As demonstrated in (Fig. 3.7) an incubator/plate reader can provide very high resolution estimates of total population density and composition if appropriate control cultures are grown alongside experimental cocultures, but the estimates are only approximate. Flow cytometry may estimate community composition more exactly, but sacrifices time resolution and accuracy in total population density estimation. Viable cell counting is the gold standard method for measuring viable cell counts; combined with fluorescent imaging it can provide the most exact estimates of both total population density and composition.

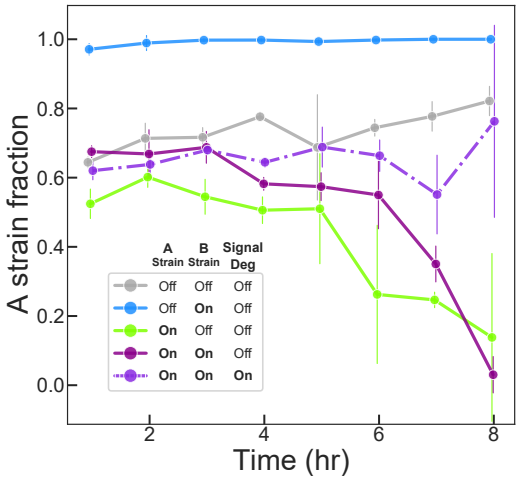

Figure 3.9: Setting composition steady states with *A=B*. A61 and B42 strains were mixed in a 1:1 ratio and grown in the indicated conditions. A strain ON = 1 mM IPTG alone; B strain ON = 30 uM Sal alone; both strain ON = 1 mM IPTG, 30 uM Sal; both ON with deg = 1 mM IPTG, 30 uM Sal, 1 mM DHBA

Because this experiment is regularly diluted, steady state population density is never achieved (Fig. 3.13), but community composition—the characteristic whose control is predicted to be most affected by AHL degradation—can be observed precisely by counting viable colony forming units of each cell strain just before each dilution.

First, the experiment clearly shows that lopsided induction of A or B cells causes the expected shift towards monoculture composition (e.g. A strain induction causes A cell death and B cell monoculture), but with different time scales. B strain induction almost immediately causes the culture to become dominated by A cells, but A strain induction only slowly decays towards B cell dominance. In our experiment testing the A61+B42 coculture's response to parallel increasing inducers, we found it decays to A strain dominance with induction. Here we demonstrate that other composition steady states are possible with different inducer concentrations.

We find regular dilution of AHL signal (and cells) is not sufficient to prevent a coculture's runaway towards monoculture. Even with maximal induction of both A and B strains, the population still slowly decays towards B strain monoculture. The coculture is clearly not stable compared to the control uninduced culture, which, as expected, maintains a stable composition throughout the experiment despite the regular dilutions.

In our previous experiment, the opposite trend was observed, maximal induction of A and B strains produced a shift towards A strain monoculture. The previous experiment was only allowed to grow through 2 complete growth cycles, where the cocultures in this experiment were regularly diluted to allow constant growth. It is possible that with more growth cycles, an A strain dominated A61+B42 coculture would eventually decay to B strain dominance as well.

When both A and B strains are maximally induced, *and* aiiA is induced, the coculture behaves as if no AHL is present at all, like in the control coculture. The results suggest that we may have entered the regime of *over*degradation of AHL in which strong aiiA expression causes the population to degrade AHL signals faster than it produces them, blocking all $A{=}B$ circuit effects on population composition. Further experimentation with intermediate levels of aiiA expression seems likely to allow customizable rates of AHL degradation in arbitrary environments.

3.3 Discussion

Using the *cap and release* population control motif, we created an engineered two-strain bacterial community capable of regulating both its composition and total population density to desired steady states. Toxin produced in-*cis* and antitoxin produced in-*trans* sequester each other to implement a pseudo-integral controller in the most stable circuit architecture for controlling community composition composition.

To search this system's large, multidimensional parameter space to find functional circuits, we created pools of strain variants and screened their mixtures, finding population density regulation to be a much more robust behavior to parameter variation, while composition control was rarer to find.

Experiments and model exploration revealed the critical need for degradation of the AHL signals that transfer information around the circuit. Saturation of AHL signals leads to very slow establishment of composition steady states incomplete rejection of perturbations to composition in simulation.

Periodic physical removal of AHL signals via dilution was insufficient to solve the

problem of AHL saturation; only strong expression of the aiiA lactonase enzyme could remove AHL at an appropriate rate.

This work is a basic demonstration of multi-strain community control using our circuit motif. With 3 inducers and a need to explore responses to perturbation, there is a lot of experimental space to cover to fully characterize this *A=B* circuit. Future work will explore all the various combinations of strain inducers and AHL degradation inducer to appropriately map the functional ranges available to this system. Additional experiments that perturb composition steady states are also necessary to verify the hypothesis that strong AHL degradation is critical to composition perturbation rejection by this circuit.

This successful use of the *cap and release* motif to make a functioning two-strain control circuit is exciting proof of the modularity of the motif. The *A=B* circuit is just one of many multi-strain circuit architectures *cap and release* makes available. We hope it provides a useful building block for bacterial community engineering work.

3.4 Materials and Methods

E. coli cell strains

The base *E. coli* strain used is the "Marionette Wild" strain from Meyer *et. al.* [34]. This cell strain was used to generate the A and B strain variants (Fig. 3.6) that yielded the chosen variants A61, B21 and B41, used in the experiments presented in Figures 3.7 and 3.9.

DB3.1 ccdB-resistant *E. coli* were used to amplify and purify ccdB containing A2 and B2 plasmids. These cells contain the mutant gyrA462 DNA gyrase, rendering them resistant to ccdB toxicity. DB3.1 cells were obtained from the Belgian Co-ordinated Collections of Microorganisms, accession number LMBP 4098. DB3.1 was originally sold by Invitrogen, but has been discontinued as a product.

The method of preparing *A=B* cell lines is specifically designed to minimize loss of circuit function in the resulting cells. Whenever a strain must be transformed with plasmids containing the ccdB toxin and ccdA, the base strain should be transformed first with the plasmid containing ccdA. This singly transformed cell line should then be prepared for transformation a second time with the ccdB containing plasmid. This process avoids exposing cells to leaky ccdB expression without protection by ccdA.

Plasmids and plasmid construction

Each cell line contains 2 plasmids A/B 1 and A/B 2, described below. All plasmids were assembled using the method detailed in *Halleran et al.* [12]. All inducible promoter sequences are taken from *Meyer et al.* [34] to make use of the optimized expression characteristics between the Marionette transcription factors and their associated evolved promoters. All parts are sourced from the Murray Lab parts library (Addgene Kit 1000000161 "CIDAR MoClo Extension, Volume I").

A1 and B1 plasmids contain a ccdA expression unit and an AHL synthase. They replicate using a low-copy ColE1 origin and express kanamycin resistance. The specific constructs are detailed below in the format (promoter - ribosome binding site - CDS - terminator / ...)

plasmid A1:

pLuxB - BCD8 - ccdA - L3S3P11

pTac - B0034 - CinI - ECK120029600

plasmid B1:

pCin - BCD8 - ccdA - L3S3P11(modified)

pSalTTC - B0034 - LuxI - ECK120029600

A2 and B2 plasmids contain a ccdB expression unit and a constitutively expressed fluorescent tag. They replicate using a low-copy pSC101 origin and express chloramphenicol resistance. These plasmids were assembled using a pool of ribosome binding sites (*ARL*), the Anderson RBS pool (link), such that cells transformed with the plasmid assembly each contain a different RBS. These unique plasmid variants were initially transformed into DB3.1 *E. coli* to allow amplification of the ccdB containing plasmids without risk of mutation, purified and sequenced, then transformed into Marionette Wild cells containing the appropriate A2 or B2 plasmid.

plasmid A2:

pCin - *ARL* - ccdB - B0015 /

J23100 - BCD6 - CFP - L3S3P11

plasmid B2:

pLuxB - *ARL* - ccdB - B0015 /

J23100 - BCD6 - sfYFP - L3S3P11

Cell growth experiments

Screening for functioning A and B cell variants

A and B strain variants were grown from *freshly transformed* colonies (see note about preparation in "*E coli* cell strains" in LB medium to OD600 0.3

These low density outgrowths were then mixed in all possible combinations in a 1:5 A:B ratio into fresh LB media with half-strength kanamycin (25μg/mL) and chloramphenicol (12.5μg/mL) and aliquoted in triplicate in 500μL into a square 96 well Matriplate (dot Scientific, MGB096-1-1-LG-L) pre-loaded with chemical inducers. A Labcyte Echo 525 Liquid Handler was used to aliquot inducers into each well of the plate before cell suspensions were added. Induced/"ON" mixtures were induced with 1mM IPTG and 30μM Sal, while uninduced/"OFF" mixtures received no inducers.

The plate was incubated for 23 hours in a Biotek Synergy H2 incubator/plate reader at 37°C with maximum linear shaking while OD600 and fluorescence measurements were taken every 10 minutes.

At hours 0, 7, 19, 23, 10μL of mixed culture in each well was sampled into 15% glycerol and frozen at -80°C for community quantification by flow cytometry

A note on strain numbers: strain A61 was not the 61st A strain tested, not was B42 the 42nd. 4 variants of both A and B strains were generated by transforming 4 unique A2 and B2 plasmids into cells already containing A1 and B1. 2 presumably identical colonies were taken from each of these transformations, for a total of 8 A and B strain variants each. Not all of these 8 variants grew up overnight for use in screening, leaving us with the 4 A and B strain variants presented here. 2 presumed identical clones of each A and B cell variant were taken for experimentation in case one clone failed to outgrow, or one clone had lost population control capacity by the time of the experiment.

A=B community induction with dilution

An A cell and a B cell variant were separately grown to OD 0.3 from a *freshly transformed* plate of cells containing both A/B1 and A/B2 plasmids (e.g. A1 plasmid + A2 plasmid version 61)

These low density outgrowths were mixed in all possible combinations into fresh LB media (half-strength kanamycin (25μg/mL) and chloramphenicol (12.5μg/mL)) in a 1:1 A:B ratio.

Mixtures were aliquoted in triplicate in 500μL into a square 96 well Matriplate containing inducers pre-pipetted into the plate using the Labcyte Echo. The plate was incubated for 18 hours in a Biotek Synergy H2 incubator/plate reader at 37°C with maximum linear shaking while OD600 and fluorescence measurements were taken every 10 minutes. At 18 hours, the plate was removed from the incubator, 90% of the contents of each well was removed, the Labcyte Echo 525 was used to pipet new inducer at each well's original inducer concentration, and fresh LB medium was added up to 500μL, yielding a 10x culture dilution into identical inducer conditions.

At hours 0, 18, 18 post-dilution, 25 and 43.5, the mixed culture in each well was sampled into 15% glycerol and frozen at -80°C for colony counting.

A=B coculture with regular dilutions and aiiA degradation

The A61 strain and B42 strain were separately grown to OD 0.3 from a *freshly transformed* plate of cells containing both A/B1 and A/B2 plasmids (e.g. A1 plasmid + A2 plasmid version 61).

These low density outgrowths were then mixed into fresh LB media (half-strength kanamycin (25μg/mL) and chloramphenicol (12.5μg/mL)) in all possible combinations in a 1:1 A:B ratio.

Mixtures were aliquoted in triplicate in 500μL into a square 96 well Matriplate containing inducers pre-pipetted into the plate using the Labcyte Echo 525. DHBA inducer was added manually to each well since it is dissolved in ethanol and is not pipetted accurately by the Echo.

The plate was incubated for 8 hours in a Biotek Synergy H2 incubator/plate reader at 37°C with maximal linear shaking while OD600 and fluorescence measurements were taken every 10 minutes. Every hour, the plate was removed from the incubator, half of the contents of each well were removed, and fresh LB medium with identical inducer concentrations was added up to 500μL, yielding a 2x culture dilution into identical inducer conditions. Before each dilution the culture in each well was sampled into 15% glycerol and frozen at -80°C for colony counting.

Density and Composition quantification

Flow cytometry Frozen cell samples were diluted 30x into PBS buffer containing Syto 62 nuclear stain (Thermo S11344) and incubated on ice for 30 minutes. These samples were then analyzed on a Miltenyi MACSQuant flow cytometer using the mKate/APC channel to detect Syto labeled cells from detector noise, GFP channel

to detect YFP and the CFP channel to detect CFP. FCS files were unpacked to pandas dataframes using the *fcsparser* [87] python package.

The *scikit learn* package *GaussianMixture* was used to train a double-peaked GMM model on the YFP channel of each culture's dataset. This package automatically assigns data points to the peaks in the model, allowing us to classify each cytometry event as a YFP^+ event or YFP^- event.

Colony counting Frozen cell samples were diluted 4 times to final dilutions between 10x - 10^4x into fresh LB media, then 10μL of each diluted suspension was spread on LB agar petri dishes. These plates were incubated at 37°C overnight, then colonies were counted. The number of colonies grown was multiplied by the dilution factor to obtain cells/mL.

Modeling and simulations

Mathematical model

The description of the model species and the model parameters are given in Tables (3.4, **??**) respectively. Note that the subscripts 1 and 2 in the model correspond to the cell strains A and B respectively. Parameter guesses for the inducers, the signals, and the promoter strengths were taken from [34].

Table 3.4: Model species

Species	Description
C_1	Cell type 1 (C_1) population count
C_2	Cell type 2 (C_2) population count
T_1	Average toxin (ccdB) con. in C_1 population
T_2	Average toxin (ccdB) con. in C_2 population
A_1	Average anti-toxin (ccdA) con. in C_1 population
A_2	Average anti-toxin (ccdA) con. in C_2 population
S_1	Signal 1 (S_1), Lux con. in environment
S_2	Signal 2 (S_2), Cin con. in environment

Simulations

All simulations of the ODE model were performed using the Python SciPy library [88].

3.5 Supplementary Material

Table 3.5: Model parameters

Parameter	**Description**	**units**	**value**
k_C	cell growth rate	hr$^-$1	0.897
C_{max}	carrying capacity	mL$^-$1	1.16e9
d_c	death rate constant ccdB	mL×hr^-1	0.4
k_{tox}	binding constant of ccdB	nM	1
β_{tac}	Max transcription rate, pTac	nM×hr^-1	4.8e-06
l_{tac}	leak rate, pTac	nM×hr^-1	β_{tac} / 320
k_{tac}	activation constant, pTac	uM	190
d_s	Environmental degradation constant of AHL	hr^-1	0.891
d_{sc}	Enzymatic AHL degradation constant	mL×hr^-1	(-) 0; (+) 1e-8; (+++) 1e-7
β_{sal}	Max transcription rate, pSal	nM×hr^-1	3e-06
l_{sal}	leak rate, pSal	nM×hr^-1	β_{sal} / 760
k_{sal}	activation constant, pSal	uM	29
β_{S1}	Max transcription rate, pCin	nM×hr^-1	5
l_{S1}	leak rate, pCin	nM×hr^-1	β_{S1} / 340
k_{S1}	activation constant, pCin	nM	250
k_{on}	ccdA/ccdB binding rate	$nM^{-1}hr^{-1}$	300
d_t	protein degradation rate	hr^-1	2
β_{S2}	Max transcription rate, pLux	nM×hr^-1	5
l_{S2}	leak rate, pLux	nM×hr^-1	β_{S2} / 480
k_{S2}	activation constant, pLux	nM	100
I	IPTG inducer concentration	uM	0-1000
Sal	Sal inducer concentration	uM	0-30

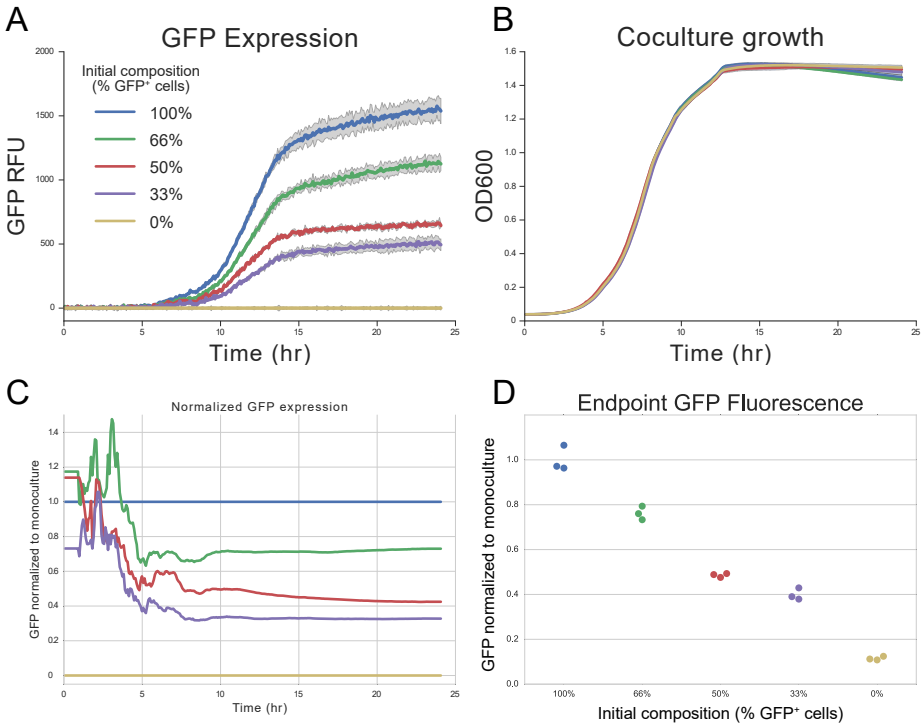

Figure 3.10: Open loop coculture growth *E. coli* labeled with either GFP or RFP were mixed in the indicated compositions, then allowed to grow over a growth cycle. Over the course of this growth, the cocultures maintained their initial compositions, as computed using GFP fluorescence normalized to the monoculture GFP$^+$ condition. (A) GFP fluorescence units, background GFP fluorescence from monoculture RFP$^+$ condition subtracted from all values. (B) Growth curves of each culture measured by OD600. (C) GFP values normalized at each time point to the monoculture GFP$^+$ condition. Estimates composition over time. (D) Endpoint GFP values normalized to the monoculture GFP$^+$ condition. Initial seeding composition appears to be maintained.

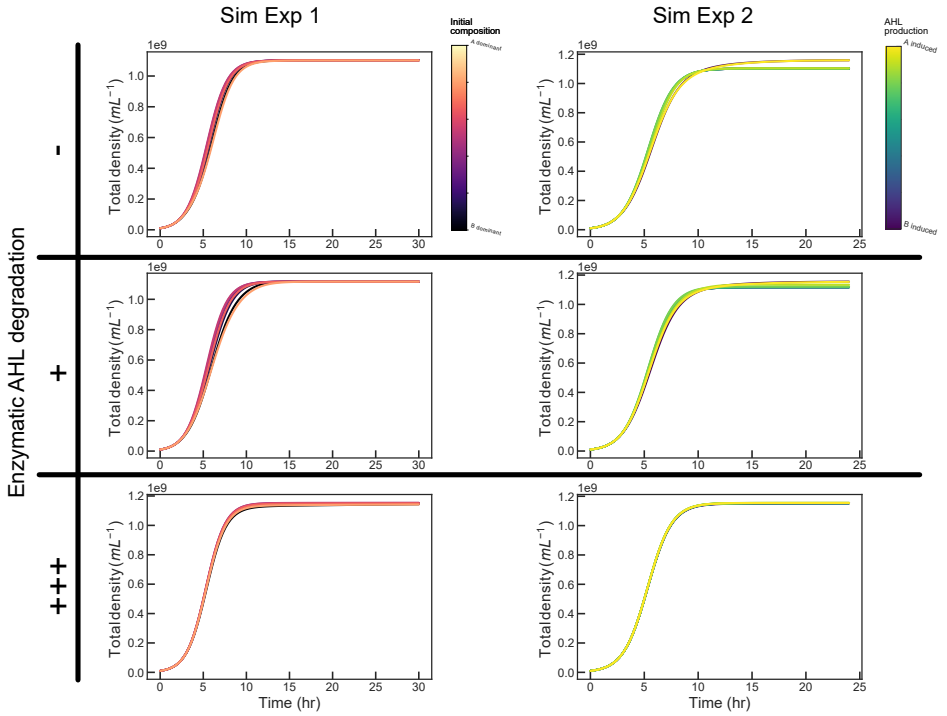

Figure 3.11: *A=B* Total population dynamics in simulated experiments For both simulated experiments (1: varying coculture initial composition, constant strong AHL production from each strain; 2: constant 1:1 initial composition, varying AHL production rates), total population dynamics do not vary significantly in response to AHL degradation rate, initial composition, or AHL production rates from both strains.

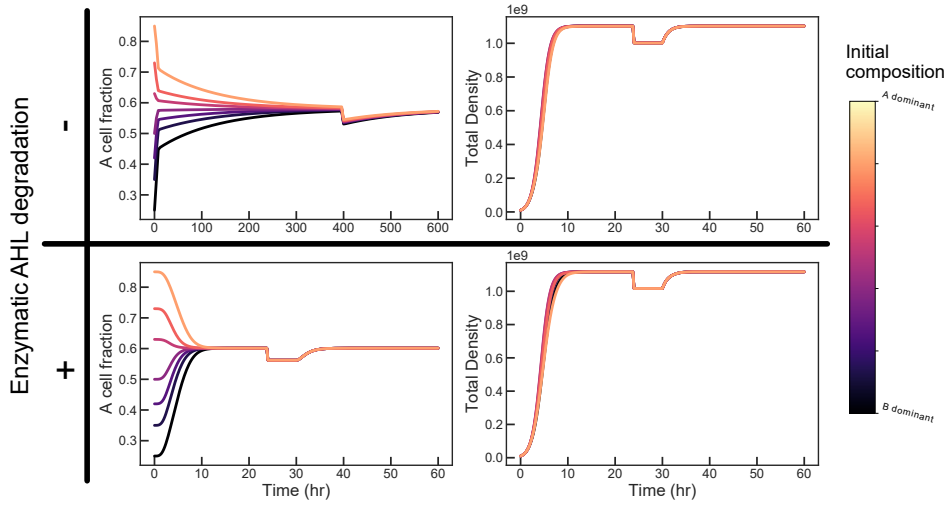

Figure 3.12: Effect of AHL degradation on perturbation rejection While AHL degradation does not appear to be required to reject disturbances in population density steady state, strong AHL degradation is required to allow the *A=B* system to respond to perturbations on reasonable timescales. The timescale on the simulation of population composition without AHL degradation is greatly extended to allow the system to achieve steady state (approx. 400 hours), so the slow response to composition perturbation (approx. 200 hours) is more clear.

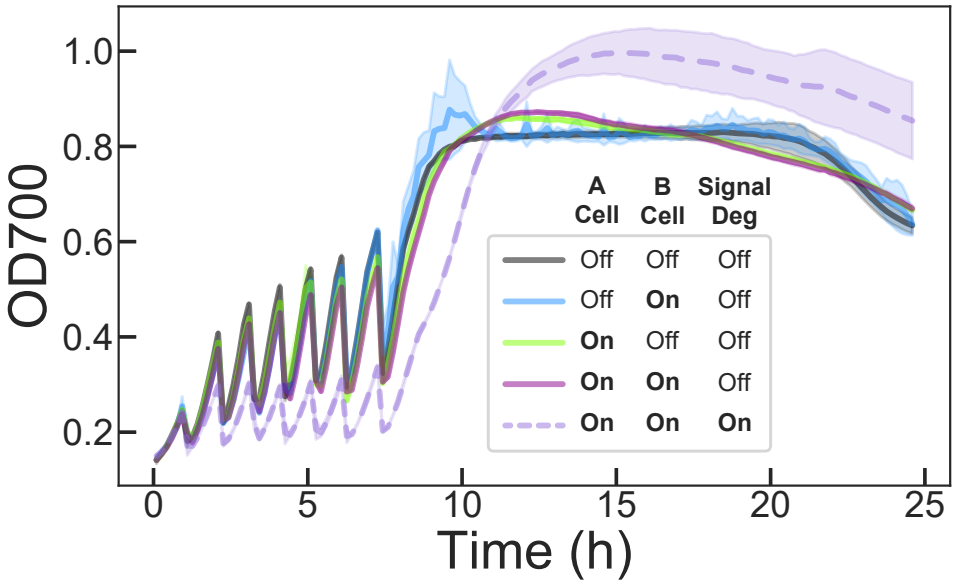

Figure 3.13: Population density dynamics in a regularly diluted *A=B* experiment Every hour, the A61+B42 strain coculture was diluted 1:2 with fresh medium containing identical inducer concentrations. Population steady state is never achieved, but composition is allowed to progress to steady state through many cycles of log phase growth.